

Coordinated glucose-induced Ca^{2+} and pH responses in yeast *Saccharomyces cerevisiae*

Tien-Yang Ma^{a,b}, Marie-Anne Deprez^b, Geert Callewaert^{a,*}, Joris Winderickx^{b,*}

^a The Yeast Hub Lab, KU Leuven, Campus Kulak, Etienne Sabbelaan 53, 8500 Kortrijk, Belgium

^b Functional Biology, Department of Biology, KU Leuven, Kasteelpark Arenberg 31, 3001 Heverlee, Belgium

ARTICLE INFO

Keywords:

Yeast
Saccharomyces cerevisiae
 Ca^{2+} homeostasis
 pH homeostasis
 Glucose signaling

ABSTRACT

Ca^{2+} and pH homeostasis are closely intertwined and this interrelationship is crucial in the cells' ability to adapt to varying environmental conditions. To further understand this Ca^{2+} -pH link, cytosolic Ca^{2+} was monitored using the aequorin-based bioluminescent assay in parallel with fluorescence reporter-based assays to monitor plasma membrane potentials and intracellular (cytosolic and vacuolar) pH in yeast *Saccharomyces cerevisiae*. At external pH 5, starved yeast cells displayed depolarized membrane potentials and responded to glucose re-addition with small Ca^{2+} transients accompanied by cytosolic alkalinization and profound vacuolar acidification. In contrast, starved cells at external pH 7 were hyperpolarized and glucose re-addition induced large Ca^{2+} transients and vacuolar alkalinization. In external Ca^{2+} -free medium, glucose-induced pH responses were not affected but Ca^{2+} transients were abolished, indicating that the intracellular $[\text{Ca}^{2+}]$ increase was not prerequisite for activation of the two primary proton pumps, being Pma1 at the plasma membrane and the vacuolar and Golgi localized V-ATPases. A reduction in Pma1 expression resulted in membrane depolarization and reduced Ca^{2+} transients, indicating that the membrane hyperpolarization generated by Pma1 activation governed the Ca^{2+} influx that is associated with glucose-induced Ca^{2+} transients. Loss of V-ATPase activity through concanamycin A inhibition did not alter glucose-induced cytosolic pH responses but affected vacuolar pH changes and Ca^{2+} transients, indicating that the V-ATPase established vacuolar proton gradient is substantial for organelle H^+ / Ca^{2+} exchange. Finally, a systematic analysis of yeast deletion strains allowed us to reveal an essential role for both the vacuolar H^+ / Ca^{2+} exchanger Vcx1 and the Golgi exchanger Gdt1 in the dissipation of intracellular Ca^{2+} .

Abbreviations

TECC, transient elevation of cytosolic calcium;
 $[\text{Ca}^{2+}]_{\text{cyt}}$, cytosolic calcium concentration;
 pH_{cyt} , cytosolic pH;
 pH_{vac} , vacuolar pH;
 D, synthetic dextrose;
 DiSC₃(3), 3,3-Dipropylthiadicarbocyanine iodide

1. Introduction

Cells have evolved a sophisticated sensing and signaling system to adapt to environmental changes, such as fluctuations in temperature, pH, osmotic pressure or nutrient availability. In eukaryotes, Ca^{2+} acts as an intracellular messenger regulating a myriad of biological processes, including exocytosis, cell proliferation, apoptosis, cell survival and

muscle contraction [1–4]. Also yeast cells employ a complex Ca^{2+} signaling network to respond to diverse external stimuli. In the budding yeast *Saccharomyces cerevisiae*, intracellular Ca^{2+} responses have been observed upon exposure to mating pheromone [5–7], hypo- or hyperosmotic stress [8, 9], alkaline stress [10], cold stress [11], toxic metal ions [12, 13]. In addition, the availability of the fermentable sugar glucose has been extensively studied ever since it was shown that refeeding of glucose to glucose-starved cells triggers a rapid, transient increase in Ca^{2+} influx [14, 15].

In *S. cerevisiae* cells, the cytosolic free Ca^{2+} concentration ($[\text{Ca}^{2+}]_{\text{cyt}}$) is normally maintained at very low levels (50–200 nM), which is 10^2 – 10^4 times lower than the external $[\text{Ca}^{2+}]$ or the free $[\text{Ca}^{2+}]$ stored in intracellular organelles [16] (estimated at 300 μM , 10 μM and 30 μM in Golgi [17], endoplasmic reticulum (ER) [18] and vacuole [19], respectively). This steep Ca^{2+} gradient between cytosol and extracellular fluid and intracellular organelles allows the generation of rapid

* Corresponding author.

E-mail addresses: geert.callewaert@kuleuven.be (G. Callewaert), joris.winderickx@kuleuven.be (J. Winderickx).

<https://doi.org/10.1016/j.ceca.2021.102479>

Received 2 June 2021; Received in revised form 23 September 2021; Accepted 24 September 2021

Available online 26 September 2021

0143-4160/© 2021 The Authors.

Published by Elsevier Ltd.

This is an open access article under the CC BY-NC-ND license

(<http://creativecommons.org/licenses/by-nc-nd/4.0/>).

changes in $[Ca^{2+}]_{\text{cyt}}$ in response to stresses or stimuli, and this is dynamically regulated by a calcineurin-dependent feedback control system consisting of various Ca^{2+} transporters, Ca^{2+} binding proteins and regulators [7].

Re-addition of glucose to glucose-starved yeast cells results in a variety of effects including the aforementioned transient elevation of cytosolic Ca^{2+} , which is known as the TECC response [14, 15, 20]. This TECC response mainly relies on Ca^{2+} influx from the external medium, followed by a rapid sequestration of the cytosolic Ca^{2+} in organelles. The Ca^{2+} influx is activated through the Glucose Induced Calcium (GIC) pathway that involves an as-yet unidentified transport system [21]. The subsequent sequestration of cytosolic Ca^{2+} , has mainly been ascribed to the vacuole-localized Ca^{2+}/H^+ antiporter Vcx1, which rapidly restores the brief cytosolic Ca^{2+} burst to non-toxic levels [22–24]. This transient increase in $[Ca^{2+}]_{\text{cyt}}$ further results in the activation of the calmodulin/calcineurin signaling pathway, which provides the transcriptional feedback regulation for a number of genes, including *PMCI* and *PMR1* [25–27]. *PMCI* encodes a vacuole-localized Ca^{2+} pump that is responsible for maintaining basal $[Ca^{2+}]_{\text{cyt}}$ [28], while *PMR1* encodes a Golgi-localized Ca^{2+} pump [29, 30], which together with the Golgi-resident Ca^{2+}/H^+ antiporter Gdt1 [31, 32] supplies the Golgi apparatus and ER with adequate levels of $[Ca^{2+}]$. In addition, it has been shown that calcineurin effectively inhibits Vcx1 providing bi-stability in cytosolic Ca^{2+} levels [24, 27, 33].

In addition to the TECC responses, glucose refeeding to yeast cells also induces an initial cytosolic acidification, followed by a more pronounced and long-lasting alkalization [14]. The initial acidification is apparently related to the release of protons (H^+) during subsequent glucose phosphorylation steps [34], while the alkalizing component is thought to be mainly caused by a glucose-induced activation of the plasma membrane H^+ -ATPase (Pma1) [35]. Pma1 is considered as a master regulator of pH_{cyt} and plasma membrane potential [36]. Its glucose-induced activation was proposed to be based on Ca^{2+} and post-translational phosphorylation. The increase in $[Ca^{2+}]_{\text{cyt}}$ upon re-addition of glucose activates the serine-protease Lpx1, which through degradation of acetylated tubulin bound to Pma1 would provide access for specific protein kinases (e.g. Ptk2) that phosphorylate and activate Pma1 [37, 38]. It has been shown that *pma1* mutants exhibit Ca^{2+} sensitivity and decreased intracellular Ca^{2+} levels [39], suggesting that Pma1 is also indirectly involved in Ca^{2+} sequestration. Additionally, constitutive overexpression of calcineurin in yeast results in a *pma1* mutant phenotype, suggesting that calcineurin may negatively regulate Pma1. However, some data suggest that calcineurin may promote Pma1 activation through the gene *SIA1*, encoding a Pma1 activator [40, 41].

In addition to Pma1, V-ATPases are also central players in cellular pH homeostasis. V-ATPases are mainly found in vacuolar (the Vph1-containing V-ATPase) and Golgi (the Stv1-containing V-ATPase) membranes. V-ATPases are structurally organized in two large sectors, V0 and V1, that can rapidly disassemble or reassemble in response to external stressors [42]. During glucose starvation the vacuolar V-ATPase, but not the Golgi V-ATPase, disassembles and a fast reassembly is seen upon glucose re-addition [42]. The V-ATPase activity generates large electrochemical proton gradients and this is crucial for a number of secondary active transport systems, including the H^+/Ca^{2+} exchange mediated by the vacuolar Vcx1 and the Golgi Gdt1 antiporters. Acute inhibition of V-ATPases by concanamycin A [43] or bafilomycin A1 [22] impairs Ca^{2+} recovery and confers sensitivity to extracellular pH and Ca^{2+} in yeast. It has been proposed that Pmc1 could compensate for the loss of the Vcx1 function in a *vcx1Δ* or a *vma2Δ* mutant, the latter lacking a functional V-ATPase [43, 44]. In addition, a calcineurin-mediated internalization of Pma1 has been observed in V-ATPase mutants [45]. Accordingly, calcineurin inhibition increases the pH and Ca^{2+} sensitivity of V-ATPase mutants [46]. Moreover, calcineurin mutant strains exhibited lower V-ATPase activity during glucose deprivation at elevated external pH, suggesting that under certain conditions calcineurin may also be involved in V-ATPase

activation [47].

Clearly, studying the basic mechanisms underlying Ca^{2+} and pH changes in response to re-addition of glucose to starved yeast cells is key to the understanding of the crosstalk between Ca^{2+} and pH homeostasis. While most previous studies have focused either on cytosolic Ca^{2+} alone or on cytosolic pH, we opted to combine an aequorin-based bioluminescent assay for monitoring cytosolic Ca^{2+} with a fluorescence reporter-based assays to monitor the plasma membrane potentials and intracellular cytosolic and vacuolar pH. We show that the glucose-induced Ca^{2+} influx is not a prerequisite for Pma1 or V-ATPase activation but instead demonstrate that membrane hyperpolarization generated by Pma1 activation governs the Ca^{2+} influx associated with the TECC responses in *S. cerevisiae*. Additionally, changes in the environmental pH had markedly different effects on glucose-induced intracellular Ca^{2+} and pH responses. Our results further support that V-ATPases are the main H^+ pumps for organellar acidification, while Pma1 mainly controls the cytosolic pH and the membrane potential. Finally, a systematic analysis of yeast deletion strains allowed us to reveal an essential role for both Vcx1 and Gdt1 in the dissipation of intracellular Ca^{2+} .

2. Materials and methods

2.1. Yeast Strains, plasmids, and cell growth conditions

Yeast strains and oligonucleotides used in this study are listed in Table S1 and S2. All yeast strains were derived from the BY4741 strain (Table S1) and contained the same auxotrophic markers. The *vcx1Δgdt1Δ* strain was constructed using a modified CRISPR/Cas9 protocol [48]. Briefly, the synthetic gRNA expression cassette flanked by ribozyme and *BsaI* restriction sites was modified to include a short DNA fragment containing two *SapI* restriction sites (gblockSAPI) and cloned into the pUDP002 plasmid (Addgene Plasmid #103872), generating the pUDP002-*SapI* plasmid. This plasmid was then used to generate a gRNA entry plasmid. The 20-bp cas9 gRNA target sequence, repair DNA fragment (*vcx1repairFw* and *vcx1repairRv*) and diagnostic primers (*vcx1dgFw* and *vcx1dgRv*) were designed using the Yeastriction toolkit (<http://yeastriction.tnw.tudelft.nl>). For integration into pUDP002-*SapI*, target sequences were flanked by 3 extra nucleotides 'GTC' and 'GTT' at 5' and 3' ends, respectively (*vcx1gRNAFw* and *vcx1gRNARv*). These modified target sequences for *VCX1* deletion were then annealed to generate double-strand DNA fragments with 3-bp overhangs and cloned into the *SapI*-digested pUDP002-*SapI* to generate pUDP002-*Vcx1*. To construct the *vcx1Δgdt1Δ* strain, the pUDP002-*vcx1* and repair DNA fragment were co-transformed into *gdt1Δ* and further analysed by diagnostic primers. The *avt3Δavt4Δ* strain was constructed by crossing different mating type mutants [49]. In short, diploids generated by crossing BY4741 single-gene mutants of *avt3Δ* (*MATα*) and *avt4Δ* (*MATα*) were grown in YPD medium (2% peptone, 1% yeast extract and 2% glucose). Cells were harvested in early stationary phase and sporulated on solid medium (1% potassium acetate, 1.5% agar, pH6) for 5-6 days. Sporulated cells were resuspended in sterile water containing 0.02 mg/ml lyticase and incubated for 10 min at room temperature. Tetrad dissection was carried out on a YPD plate using a micromanipulator (Singer instruments). After incubation for 3-5 days at 30°C, genotypes of the germinated spores were analyzed. Non-transformed yeast cells were cultured and maintained in YPD medium. For Ca^{2+} measurements, the yeast strains used were transformed with the episomal plasmid pYX212-cytAeq allowing for apoaequorin expression. For cytosolic pH measurements, the strains were transformed with the episomal plasmid pYES2-*PACT1*-pHluorin. For vacuolar pH and plasma membrane potential measurements, the strains were transformed with the empty plasmid pYX212. Since all plasmids allowed for expression of *URA3*, all strains displayed the same auxotrophies for the different measurements. The transformed yeast cells were selected, cultured and maintained in synthetic dextrose (SD) minimal medium lacking uracil

(0.19% yeast nitrogen base without amino acids, 0.5% ammonium sulfate supplemented with synthetic drop-out amino acid/nucleobase mixture and 2% glucose). Glucose starvation was carried out according to Wilms, T. *et al.* 2017 [49]. Briefly, early log phase cells were washed twice and incubated in starvation medium (0.19% yeast nitrogen base without amino acids, folic acid and riboflavin (LoFlo, Formedium), 0.5% ammonium sulfate supplemented with synthetic drop-out amino acid/nucleobase mixture, without glucose) buffered at pH 7 or 5 for 1 hr. All cultures were shaken at 30°C and 200 rpm.

2.2. Cytosolic Ca^{2+} measurements

Cytosolic Ca^{2+} levels ($[Ca^{2+}]_{cyt}$) were measured in yeast strains expressing the bioluminescent protein apoaequorin as previously described [50]. Briefly, using the lithium/polyethylene glycol method [51] strains were transformed with pYX212-cytAEQ harboring the apoaequorin gene under the control of TPI promoter (kind gift from E. Martegani, Department of Biotechnology and Biosciences, University of Milano-Bicocca, Milan, Italy) [52] and grown in SD minimal medium at pH 5. For cell immobilization, two OD₆₀₀ units of cells harvested in the early log phase were plated on concanavalin A coated coverslips and incubated at 30°C for 1 hr. For aequorin reconstitution, immobilized yeast cells were washed twice with starvation medium at pH 7 or 5 and incubated in the same medium supplemented with 5 mM wild-type coelenterazine (Promega) at 30°C for 1 hr. After removing excess of coelenterazine by washing the coverslips with starvation medium pH 7 or 5, coverslips with attached yeast cells were placed in a thermostated perfusion chamber of a single-tube luminometer (photomultiplier tube for photon detection (Type H3460-04, Hamamatsu Photonics, Japan) positioned about 2 cm above the coverslip surface) and perfused with the required solutions at 30°C. In Ca^{2+} and glucose pulse experiments, immobilized cells were initially perfused with 0.1 M 2-(N-morpholino) ethanesulfonic acid (MES)/Tris buffer (Sigma) at pH 7 or 5, followed by the same buffer supplemented with 10 mM $CaCl_2$. After the Ca^{2+} pulse, cells were subsequently perfused with the same buffer supplemented with 110 mM glucose to induce a transient elevation of cytosolic calcium (referred to TECC response). In Ca^{2+} -free experiments, the same procedure was used except that 3 mM Ethylene glycol-bis(2-aminoethyl ether)-N,N,N',N'-tetraacetic acid (EGTA) (Sigma) was added to the buffer medium and the 10 mM $CaCl_2$ pulse was omitted. In the V-ATPase inhibition experiments, cells were pretreated with 1 μ M concanamycin A (CMA - Biviotica) for 15 min and then washed twice with MES/Tris buffer prior to Ca^{2+} and glucose pulse experiments. CMA was dissolved in dimethyl sulfoxide (DMSO) and cells pretreated with vehicle (1%) alone served as control. At the end of all experiments, the residual reconstituted aequorin was completely discharged by perfusing the cells with a solution containing 10 mM $CaCl_2$ and 0.5% Triton X-100. Light impulses originating from the entire yeast cell population were discriminated, pre-scaled and integrated (1 s time interval) with a PC-based 32-bit counter/timer board (PCI-6601, National Instruments Corporation, Austin, TX, United States). The emitted light was calibrated offline into cytosolic Ca^{2+} values using the following algorithm $[Ca^{2+}]_{in} = ((L/L_{max})^{1/3} + [KTR(L/L_{max})^{1/3} - 1]/(KR(L/L_{max})^{1/3})]$ with KTR and KR the constants for the Ca^{2+} -unbound and Ca^{2+} -bound state, respectively [53], L the luminescence intensity at any time point and L_{max} the integrated luminescence [24, 53, 54]. Data presented for $[Ca^{2+}]_{cyt}$ in this study are all averages of replicate traces (mean \pm SEM with N the number of coverslips tested).

2.3. Cytosolic and vacuolar pH measurements

Cytosolic pH (pH_{cyt}) was measured in strains transformed with pYES2-*PACT1*-pHluorin encoding the pH-sensitive green fluorescent ratiometric protein pHluorin (kind gift from Dr. Gertien J. Smits, Swammerdam Institute for Life Sciences (SILS), University of Amsterdam, The Netherlands) [55]. The transformed strains were grown in the

SD minimal medium, buffered at pH 5. For glucose starvation experiments, cells were harvested in the early log phase, washed twice with the starvation medium buffered to pH 5 or 7 and incubated at 30°C for 1 hr. Glucose-starved cells were then washed twice and resuspended with 0.1 M MES/Tris buffer at pH 5 or 7, and subsequently transferred to F-bottom black 96-well microplate (Greiner Bio-One). The fluorescence intensity at excitation wavelengths 389 and 485 nm was measured at an emission wavelength of 511 nm using a Fluoroskan Ascent FL Microplate Fluorometer and Luminometer (Thermo Scientific). In a series of experiments the glucose-starvation time was prolonged to 2 hrs (data not shown). Statistical analysis using two-way Anova revealed that there were no statistically significant pH_{cyt} differences between the 1 hr and the 2 hrs glucose-starved samples of wild-type and mutant strains (p-value range between 0.069 and 0.7628).

Vacuolar pH (pH_{vac}) was measured using the cell permeant ratiometric pH indicator BCECF-AM (Calbiochem). Strains grown to early log phase in SD minimal medium were loaded with 50 μ M BCECF-AM and incubated at 30°C for 30 min. BCECF-loaded cells were then starved in starvation medium and washed with MES/Tris buffer using the same approach as for cytosolic pH measurements. The fluorescence emission was recorded at 538 nm using 440 nm and 485 nm excitation.

All pH measurements were performed at 30°C with orbital shaking at 240rpm. pH values were calibrated offline using a calibration mixture described previously [49, 55]. To avoid ammonium effects on pH (Fig. S1), all pH measurements were performed in MES/Tris buffer at pH 7 or 5. For pH measurements, the same procedures were used as for cytosolic Ca^{2+} measurements cells. Data presented for pH in this study are all averages of replicate traces (mean \pm SEM with N the number of cultures tested).

2.4. Estimations of plasma membrane potential

Optical estimation of the plasma membrane potential with the fluorescent dye 3,3-Dipropylthiacarbocyanine iodide (DiSC₃(3)) (Sigma) was done using a similar protocol as described before [56] with some modifications. Yeast cells were grown in SD minimal medium buffered at pH 5, harvested in the early log phase, washed twice with starvation medium buffered at pH 7 or 5, and then incubated at 30°C for 1 hr. Before recording, cells were washed twice with MES/Tris buffer at pH 7 or 5 and transferred into 96-well black microplates at OD₆₀₀ of 1.5. DiSC₃(3) was added at a final concentration of 0.2 μ M, and 10 μ M $BaCl_2$ was added to avoid dye surface binding [57]. After 20 min incubation at 30°C, fluorescence was followed in a BioTek Synergy H1 microplate reader at 30°C. Excitation and emission fluorescence were 531 and 549–589 nm, respectively. The 580/560 ratio was used to estimate membrane potential changes. Where specified, glucose was re-added to a final concentration of 110 mM.

2.5. Fluorescence microscopy

The V-ATPase assembly was analysed in yeast strains expressing GFP-tagged Vma2 (RD67) and grown to early log phase in SD minimal medium. Vacuolar membranes were stained with FM4-64 (Thermo Fisher) (8 μ M FM4-64 for 30 min at 30°C). For glucose starvation, cells were washed twice with starvation medium buffered at pH 7 or 5, and then incubated at 30°C for 1 hr. Before imaging, cells were washed twice with MES/Tris buffer at pH 7 or 5. Fluorescence was visualized with a Leica DM4000B or DMi8 microscope. Images were deconvolved with Huygens Essential (v18.04, Scientific Volume Imaging) and further processed with Fiji (v1.53c) [58]. $CaCl_2$ or glucose were added where indicated to a final concentration of 10 mM and 110 mM, respectively. Co-localization of Vma2-GFP with vacuolar FM4-64 was quantified using the ImageJ plugin Just Another Colocalization (JACoP) [59] to calculate the Pearson's coefficient (denoted as mean \pm SEM with N the number of cells tested).

2.6. Cell growth determination

In yeast cells undergoing acute glucose starvation growth was assessed by monitoring the optical density (OD) at 595 nm (96-well plate reader Multiskan Go, Thermo Scientific). Absorbance data were averaged for each condition and plotted as a function of time. **Fig. S2 A** shows that at pH_{out} 5 and 7 wild-type yeast cells have limited growth under glucose starvation. The doubling time for wild-type and mutant cells growing in the presence of glucose or under glucose-starvation conditions is provided in **Fig. S2 B**. Under glucose-starvation conditions at pH_{out} 5 and 7, no significant differences were observed between wild-type and mutant strains.

2.7. Glucose uptake quantification

Glucose uptake into yeast cells was quantified using the fluorescent glucose derivative 2-NBDG (2-(N-(7-nitrobenz-2-oxa-1,3-diazol-4-yl)-amino)-2-deoxyglucose) as previously described [60]. Briefly, yeast cells were incubated with 60 μM of 2-NBDG at 30°C for 30 min. The uptake reaction was stopped by washing the cells three times with MES/Tris buffer at pH_{out} 5 or 7. Live cells were visualized with a Leica DM4000B or DMi8 microscope using GFP filter. The quantification of 2-NBDG fluorescence was calculated using Fiji (v1.53c) software. At least 150 cells were analysed for each yeast strain. Normalized 2-NBDG fluorescence (the fluorescence of 2-NBDG from wild-type cells at pH_{out} 5 was set to 1.0) was plotted with data showing averages \pm SEM (**Fig. S3**).

2.8. Statistical analysis

Results are expressed as mean \pm standard error of mean (SEM). Unpaired Student's t-test was used to determine statistical significance between two datasets. The two-way analysis of variance (ANOVA) test was used to check for significant differences in pH_{cyt} between 1 hr and 2 hrs glucose-starved cells.

3. Results

3.1. Ca^{2+} signaling and pH regulation following glucose re-addition to glucose-starved yeast cells

To study the crosstalk between pH and Ca^{2+} homeostasis in yeast cells, we monitored in parallel the cytosolic pH (pH_{cyt}) and vacuolar pH (pH_{vac}) as well as cytosolic Ca^{2+} concentrations ($[\text{Ca}^{2+}]_{\text{cyt}}$) when first Ca^{2+} and then glucose were supplemented to glucose-starved yeast cells. The panels in **Fig. 1** show the changes in $[\text{Ca}^{2+}]_{\text{cyt}}$ and accompanying pH changes in wild-type BY4741 cells at an external pH (pH_{out}) of 5 and 7. The $[\text{Ca}^{2+}]_{\text{cyt}}$ baseline levels under starvation conditions were not significantly different between pH_{out} 5 and 7, while pH_{cyt} was 5.84 ± 0.04 ($N = 3$) and 5.65 ± 0.04 ($N = 3$) ($p < 0.005$), and pH_{vac} was 6.05 ± 0.04 ($N = 3$) and 5.89 ± 0.03 ($N = 4$) ($p < 0.005$) at pH_{out} 5 and 7, respectively. Addition of external CaCl_2 induced a rapid small $[\text{Ca}^{2+}]_{\text{cyt}}$ increase, which was more pronounced at pH_{out} 7, but no distinct pH changes were observed. Glucose re-addition generated the characteristic TECC response as previously reported [14, 15, 21]. At pH_{out} 7, the TECC response showed a relatively fast onset with a high peak amplitude (3.73 ± 0.31 μM , $N = 5$) that was reached at 262 s after the glucose pulse (**Fig. 1 B**), whereas at pH_{out} 5, the TECC response displayed a significant lower amplitude (0.82 ± 0.05 μM , $N = 4$), which reached a maximum at 373 s after the glucose pulse (**Fig. 1 D**). The large TECC response observed at pH_{out} 7 was accompanied by an initial and small cytosolic acidification followed by a large and prolonged cytosolic alkalinization (pH_{cyt} 6.89 ± 0.06 , $N = 3$) while the vacuolar pH increased (pH_{vac} 6.14 ± 0.07 , $N = 4$) (**Fig. 1 A**). This resulted in a vacuolar pH gradient of 0.75 pH units. The small TECC response at pH_{out} 5 was again accompanied by an initial slight pH_{cyt} decrease followed by a progressive but more modest cytosolic alkalinization (pH_{cyt} 6.20 ± 0.02 , $N = 3$) (**Fig. 1**

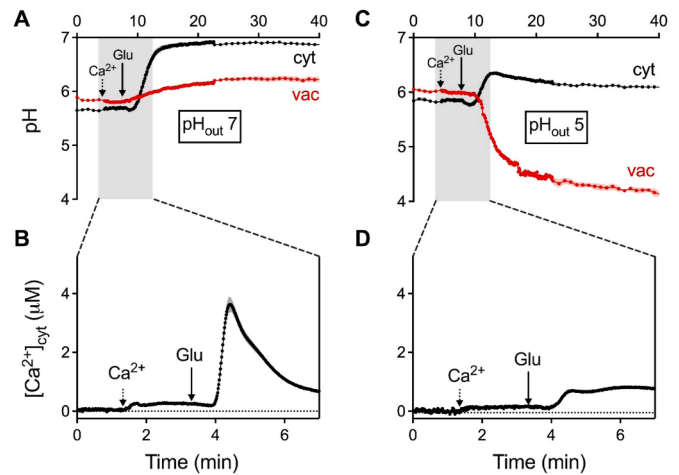


Fig. 1. Cytosolic $[\text{Ca}^{2+}]$ and pH changes in glucose-starved wild-type BY4741 yeast cells. (A and C) Averaged pH (cytosol (cyt) - black traces; vacuole (vac) - red traces) and (B and D) corresponding averaged cytosolic Ca^{2+} transient in response to a 10 mM external CaCl_2 pulse (Ca^{2+} - first dotted arrow) followed by re-addition of glucose to a final concentration of 110 mM (Glu - second arrow - TECC response) in BY4741 yeast cells kept at pH_{out} 7 (A and B) or 5 (C and D). Shaded areas either side of the $[\text{Ca}^{2+}]$ or pH data points reflect SEM.

C). However, at pH_{out} 5, glucose re-addition caused a strong acidification of the vacuole (pH_{vac} 4.46 ± 0.08 , $N = 3$), thereby creating a large vacuolar H^+ gradient of 1.74 pH units. Notably, the failure to acidify the vacuole upon glucose re-addition at pH_{out} 7 was previously reported before in a study that also demonstrated hampered V-ATPase disassembly in response to glucose deprivation at pH_{out} 7 [47].

3.2. The contribution of Pma1

The initial cytosolic acidification observed upon glucose re-addition is likely related to the release of H^+ during subsequent glucose phosphorylation steps [34], while the alkalinizing cytosolic phase might reflect the glucose-induced activation of Pma1, the plasma membrane H^+ -ATPase [35]. It has previously been proposed that the glucose-induced activation of Pma1 involves Ca^{2+} signaling since deprivation of extracellular Ca^{2+} partly inhibits its glucose-induced activity [61]. To assess whether TECC responses contribute to glucose-induced Pma1 activation, we recorded TECC and pH responses in external Ca^{2+} -free medium supplemented with EGTA (3 mM). As expected, the TECC responses, which mainly rely on Ca^{2+} influx from the external medium [21], were fully suppressed under these conditions (**Fig. 2, A and D**). Surprisingly, however, the accompanying pH_{cyt} changes were not affected both at pH_{out} 5 and 7 (**Fig. 2, B and E**). Similarly, pH_{vac} was not affected at pH_{out} 7 and only a moderate decrease in pH_{vac} was observed at pH_{out} 5 (**Fig. 2, C and F**). As expected, when glucose re-addition was omitted the TECC responses and pH changes were both eliminated (**Fig. 2**). Combined, these findings thus clearly indicate that the observed pH changes are solely glucose-dependent and that cytosolic alkalinization is not triggered by the TECC response, the latter suggesting that Pma1 activation in the present experimental conditions is not Ca^{2+} -dependent.

To further investigate the contribution of Pma1, complementary experiments were performed using the *pma1-007* mutant strain (**Fig. 3**). This strain has a small deletion in the *PMA1* promoter region that reduces the expression by about 50%. In consequence, the *pma1-007* mutant strain displays an impaired capacity to pump protons out of the cell [62]. At pH_{out} 7, the $[\text{Ca}^{2+}]_{\text{cyt}}$ and pH baseline levels (pH_{cyt} 5.83 ± 0.02 , $N = 6$; pH_{vac} 5.95 ± 0.04 , $N = 6$) under starvation conditions were remarkably similar in *pma1-007* mutant cells and wild-type

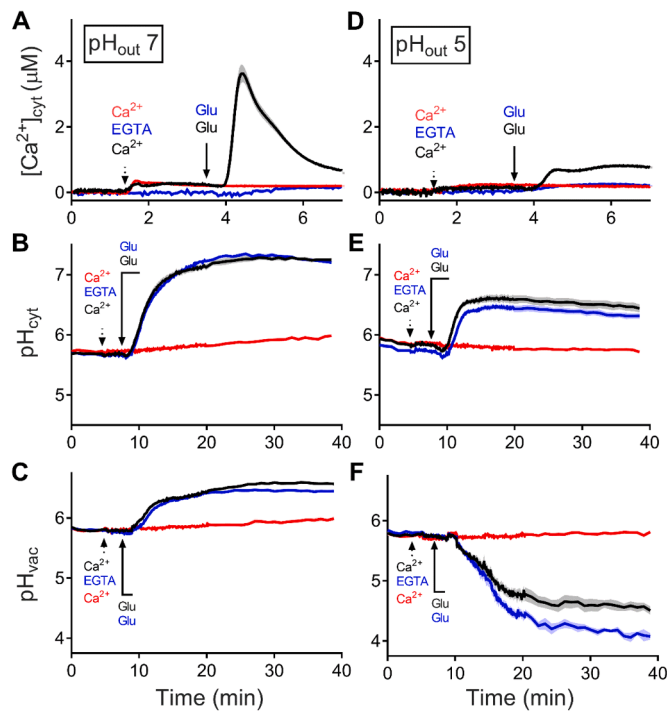


Fig. 2. Effect of external Ca^{2+} and glucose on cytosolic $[\text{Ca}^{2+}]$ and pH changes in glucose-starved wild-type BY4741 yeast cells. (A and D), cytosolic pH (B and E) and vacuolar pH (C and F) in glucose-starved BY4741 yeast cells at pH_{out} 7 (A, B and C) or 5 (D, E and F). Black traces indicate averaged $[\text{Ca}^{2+}]$ or pH in response to a 10 mM external CaCl_2 pulse (first dotted arrow) followed by re-addition of glucose to a final concentration of 110 mM (second arrow – TECC response). TECC responses and fast pH changes were completely abolished when glucose was not re-administered (red traces and labels). In yeast cells kept in Ca^{2+} -free medium supplemented with EGTA (3 mM), cytosolic $[\text{Ca}^{2+}]$ changes were completely abolished but pH changes in response to glucose re-addition were not profoundly affected (blue traces and labels). Shaded areas either side of the $[\text{Ca}^{2+}]$ and pH data points reflect SEM. Note that the pH range for cytosol and vacuole are different but the same scaling factor was used, allowing comparison of pH changes.

BY4741 cells (Fig. 3, A–C). However, following glucose re-addition, the cytosolic alkalinization was significantly slower and smaller, while the vacuolar alkalinization was more pronounced, resulting in a reduced vacuolar H^+ gradient of 0.28 pH units ($\text{pH}_{\text{cyt}} 6.73 \pm 0.09$, $N = 6$; $\text{pH}_{\text{vac}} 6.45 \pm 0.05$, $N = 6$) in the *pma1-007* mutant (Fig. 3, B and C). At pH_{out} 5, we noticed that the baseline pH_{vac} under starvation conditions was significantly lower in the *pma1-007* mutant as compared to the wild-type strain (*pma1-007*: $\text{pH}_{\text{vac}} 5.32 \pm 0.08$, $N = 6$; wild-type: $\text{pH}_{\text{vac}} 5.99 \pm 0.06$, $N = 6$) (Fig. 3 F). This vacuolar hyperacidification likely reflects compensatory effects in the *pma1-007* mutant strain to maintain variations in the pH_{cyt} within limits. Remarkably, the addition of external CaCl_2 to the *pma1-007* mutant allowed a larger $[\text{Ca}^{2+}]_{\text{cyt}}$ increase as that normally seen in the wild-type at pH_{out} 5 (Fig. 3 D), suggesting that this increase may be related to the baseline hyperacidification of the vacuole.

Upon re-supplementation of glucose, almost no additional $[\text{Ca}^{2+}]_{\text{cyt}}$ increase was observed in the *pma1-007* mutant at pH_{out} 5, while the TECC response at pH_{out} 7 was strongly reduced in comparison to the wild-type strain (Fig. 3, A and D). A TECC response reflects the delicate balance between Ca^{2+} influx, organellar sequestration and release. Based on the current data, we propose that the decreased TECC responses in the *pma1-007* mutant are primarily due to a reduced Ca^{2+} influx. As a result of its electrogenic transport of protons, Pma1 generates hyperpolarizing current over the plasma membrane when activated and therefore Pma1 activity may promote Ca^{2+} entry by increasing the electrochemical driving force for Ca^{2+} ions.

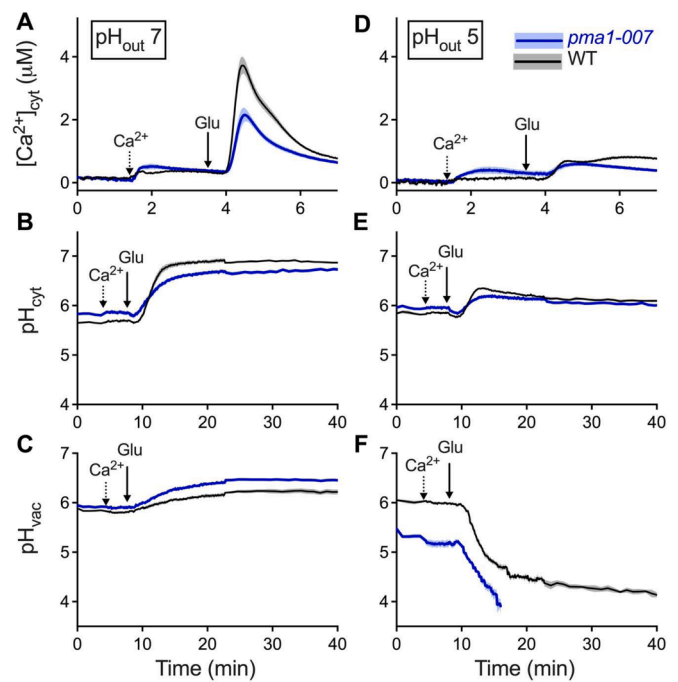


Fig. 3. Cytosolic $[\text{Ca}^{2+}]$ and pH changes in glucose-starved *pma1-007* mutant yeast cells. (A and D) Averaged cytosolic Ca^{2+} transient (blue traces) in response to a 10 mM external CaCl_2 pulse (Ca^{2+} - first dotted arrow) followed by re-addition of glucose to a final concentration of 110 mM (Glu - second arrow) in *pma1-007* mutant yeast cells kept at pH_{out} 7 (A) or 5 (D). For comparison, black traces show averaged cytosolic Ca^{2+} transient in control wild-type BY4741 cells (WT). Shaded areas either side of the Ca^{2+} transient trajectories reflect SEM. (B–C and E–F) Corresponding averaged cytosolic (B and E) and vacuolar (C and F) pH changes (blue traces in *pma1-007* mutant yeast cells kept at pH_{out} 7 (B and C) or 5 (E and F). For comparison, black traces show averaged cytosolic and vacuolar pH changes in control BY4741 cells (WT). Shaded areas either side of the pH data points reflect SEM. Note that the pH range for cytosol and vacuole are different but the same scaling factor was used, allowing comparison of pH changes.

To test whether changes in membrane potential could explain the reduced TECC responses in *pma1-007* mutants, we monitored the membrane potentials using the fluorescent voltage-sensitive probe DiSC3(3). To limit that Ca^{2+} influx would counterbalance or mask Pma1-related membrane potential changes, the experiments were conducted

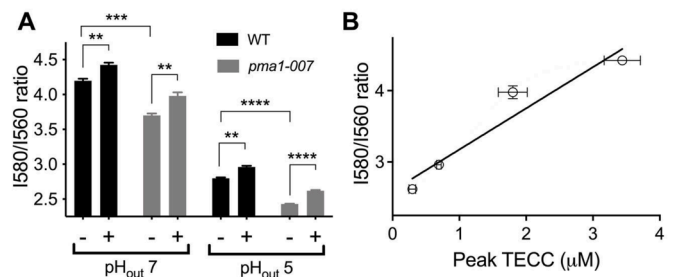


Fig. 4. Effect of membrane potential on TECC responses. Measurement of relative membrane potential of yeast cells using the 1580 / 1560 fluorescence emission ratio of diS-C3(3). (A) 1580/1560 emission ratio in control wild-type BY4741 (WT - black bars) and *pma1-007* mutant cells (grey bars) in the absence (-) or presence (+) of 110 mM glucose at pH_{out} 7 and 5 as indicated. Ratios are mean \pm SEM ($N = 4$) and ** denotes $p < 0.01$, *** $p < 0.001$, **** $p < 0.0001$. (B) Correlation between mean 1580/1560 emission ratio and mean peak $[\text{Ca}^{2+}]$ of TECC responses. Peak TECC was defined as the difference between the TECC amplitude and the $[\text{Ca}^{2+}]_{\text{cyt}}$ before glucose re-addition. Solid line: linear fit with slope 0.58 ($R^2 = 0.92$).

in Ca^{2+} -free medium supplemented with EGTA. As shown in Fig. 4 A, both at $\text{pH}_{\text{out}} 7$ and $\text{pH}_{\text{out}} 5$, the I580/I560 emission ratios of DiS-C3(3) were consistently lower in *pma1-007* cells as compared to wild-type cells, indicative for a relative membrane depolarization in the mutant (at $\text{pH}_{\text{out}} 7$: *pma1-007*: 3.70 ± 0.05 , $N = 3$; wild-type: 4.19 ± 0.05 , $N = 3$, $p < 0.001$, at $\text{pH}_{\text{out}} 5$: *pma1-007*: 2.43 ± 0.01 , $N = 3$; wild-type: 2.79 ± 0.02 , $N = 3$, $p < 0.0001$). The re-addition of glucose caused a marked increase in the emission ratios (at $\text{pH}_{\text{out}} 7$: *pma1-007*: 3.98 ± 0.09 , $N = 4$, $p < 0.01$; wild-type: 4.42 ± 0.05 , $N = 4$, $p < 0.01$; at $\text{pH}_{\text{out}} 5$: *pma1-007*: 2.62 ± 0.02 , $N = 4$, $p < 0.0001$; wild-type: 2.96 ± 0.03 , $N = 4$, $p < 0.01$), indicative that hyperpolarization of the membrane potential still occurred in both strains as reported previously [15, 63]. Note, however, that the emission ratios at $\text{pH}_{\text{out}} 5$ were consistently lower than those obtained at $\text{pH}_{\text{out}} 7$, indicating that cells become depolarized at $\text{pH}_{\text{out}} 5$. Next, we plotted the I580/I560 ratio obtained after glucose re-addition versus the peak TECC response for the *pma1-007* and wild-type strains. As shown in Fig. 4 B, these correlated well, thereby confirming that the glucose-induced Ca^{2+} influx is indeed mainly controlled by the plasma membrane potential, which is to a large extent generated by the Pma1 activity.

3.3. The contribution of the V-ATPase

In addition to Pma1, vacuolar and Golgi V-ATPases are also central players in cellular pH homeostasis. The glucose-induced strong vacuolar acidification observed at $\text{pH}_{\text{out}} 5$ is consistent with a fast reassembly and activation of the vacuolar V-ATPase [64] while the vacuolar acidification defect observed at $\text{pH}_{\text{out}} 7$ is in line with the small glucose-induced pH_{vac} increase reported previously [47]. To elaborate on this, we examined the V-ATPase assembly status by pulse-chase imaging monitoring the co-localization of GFP-tagged Vma2 and FM4-64 labelled vacuolar membranes in function of Ca^{2+} and glucose availability. This revealed that the vacuolar V-ATPase assembly status is solely dependent on glucose availability and that a similar enhanced assembly is observed at $\text{pH}_{\text{out}} 5$ and $\text{pH}_{\text{out}} 7$ (Fig. S4). This excludes that the vacuolar acidification defect at $\text{pH}_{\text{out}} 7$ would be linked to a lower V-ATPase assembly. In addition, the glucose-induced vacuolar alkalization at $\text{pH}_{\text{out}} 7$ was not prevented in deletion strains lacking proton-coupled transporters, including *vcx1Δ*, *nhx1Δ*, *vmx1Δ* and *avt3Δavt4Δ* (Fig. S5), thereby confirming again previous reported data [47] and eliminating the possibility that the vacuolar acidification defect at $\text{pH}_{\text{out}} 7$ would reflect an altered H^+ exchange transport activity.

To further address the role of the V-ATPases, yeast cells were treated with the V-ATPase inhibitor concanamycin A (CMA). In wild-type BY4741 cells pretreated with $1 \mu\text{M}$ CMA for 15 min, the steady-state pH_{vac} values attained following glucose re-addition were significantly increased at $\text{pH}_{\text{out}} 5$ and 7 , as compared to DMSO-treated control cells (at $\text{pH}_{\text{out}} 5$: $\text{pH}_{\text{vac}} 5.69 \pm 0.06$, $N = 4$, $p < 0.001$; at $\text{pH}_{\text{out}} 7$: 6.46 ± 0.11 , $N = 6$, $p < 0.001$), while pH_{cyt} values were not significantly affected (Fig. 5, B and C). The latter finding suggests that the V-ATPases contribute little to cytosolic pH regulation in response to glucose re-addition. The TECC responses at $\text{pH}_{\text{out}} 5$ and 7 were significantly enhanced in CMA-treated cells (Fig. 5, A and D). Notably, dimethyl sulfoxide (DMSO – 1%) as the solvent for CMA had no significant effects on pH (data not shown) and only a minor effect on cytosolic $[\text{Ca}^{2+}]$ (Fig. S6). Since the vacuolar and Golgi pH gradients that drive the uptake of Ca^{2+} via the $\text{Ca}^{2+}/\text{H}^+$ antiporters Vcx1 and Gdt1 are strongly reduced in CMA-treated cells, it is likely that the increased TECC responses in CMA-treated cells mainly reflect lower Vcx1- or Gdt1-mediated Ca^{2+} sequestration.

3.4. The contribution of the vacuolar and Golgi $\text{Ca}^{2+}/\text{H}^+$ antiporters Vcx1 and Gdt1

To validate the involvement of Vcx1 and Gdt1 in mediating the TECC responses, we analysed $[\text{Ca}^{2+}]_{\text{cyt}}$, pH_{cyt} and pH_{vac} in the *vcx1Δ*, *gdt1Δ*

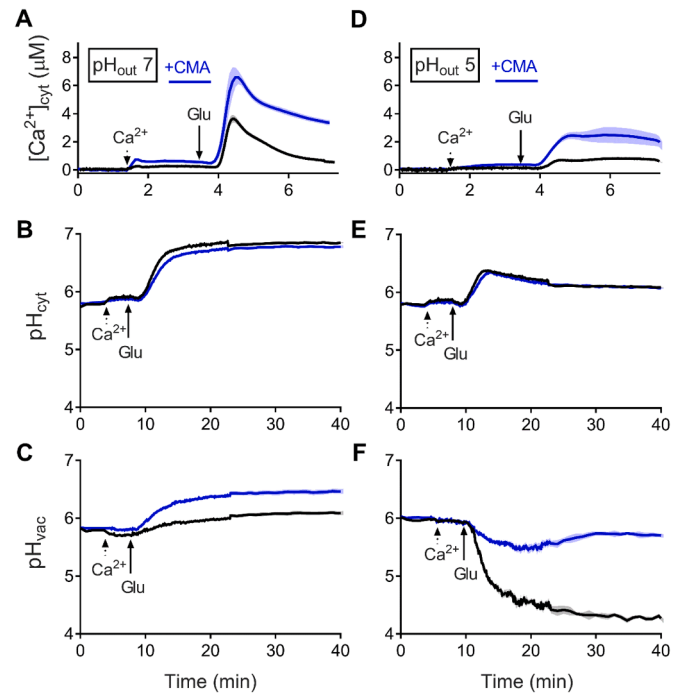


Fig. 5. Effect of the V-ATPase inhibitor Concanamycin A (CMA) on cytosolic $[\text{Ca}^{2+}]$ and pH changes in glucose-starved wild-type BY4741 yeast cells. (A and D) Averaged cytosolic Ca^{2+} transient in response to a 10 mM external CaCl_2 pulse (Ca^{2+} - first dotted arrow) followed by re-addition of glucose to a final concentration of 110 mM (Glu - second arrow) in vehicle-treated control wild-type cells (black traces) and wild-type cells pretreated with $1 \mu\text{M}$ CMA for 15 min (CMA; blue traces) and kept at external pH 7 (A) or 5 (D). Shaded areas either side of the Ca^{2+} transient trajectories reflect SEM. (B-C and E-F) Corresponding averaged pH (cytosol (cyt) - B and E; vacuole (vac) - C and F; shaded area either side of the pH data points reflects SEM) in vehicle-treated control (black traces) and cells pretreated with $1 \mu\text{M}$ CMA for 15 min (CMA; blue traces) and kept at external pH 7 (B-C) or 5 (E-F). Shaded areas either side of the pH data points reflect SEM.

and *vcx1Δgdt1Δ* strains. As shown in Fig. 6, pH_{cyt} and pH_{vac} responses at both $\text{pH}_{\text{out}} 7$ and 5 were not affected in the *vcx1Δ* strain (Fig. 6, B and D), indicating that H^+ flux via Vcx1 neither affects cytosolic or vacuolar pH homeostasis. The TECC response at $\text{pH}_{\text{out}} 7$ was clearly enhanced in the *vcx1Δ* mutant (peak amplitude: $7.55 \pm 0.27 \mu\text{M}$) as compared to the wild-type strain (peak amplitude: $3.73 \pm 0.31 \mu\text{M}$) (Fig. 6, A and C). Moreover, the $[\text{Ca}^{2+}]_{\text{cyt}}$ in the *vcx1Δ* mutant remained high in the subsequent phase measured at 3 min after glucose addition (*vcx1Δ*: $1.83 \pm 0.13 \mu\text{M}$; $N = 3$, WT: $0.69 \pm 0.04 \mu\text{M}$; $N = 5$), indicating that Vcx1 plays indeed a crucial role in the rapid dissipation of Ca^{2+} , which is in agreement with previous reports [22]. Surprisingly, at $\text{pH}_{\text{out}} 5$ the *vcx1Δ* strain showed a similar TECC response as the wild-type strain (Fig. 6 C). This is in sharp contrast to the enhanced TECC response observed in CMA-treated cells at $\text{pH}_{\text{out}} 5$ (Fig. 5 D). The findings that the organellar H^+ gradient at $\text{pH}_{\text{out}} 5$ is well preserved in *vcx1Δ* cells but greatly reduced in CMA-treated cells, raise the possibility that when the cytosolic Ca^{2+} load is limited other $\text{H}^+/\text{Ca}^{2+}$ transporters, notably the Golgi-localized Gdt1, may compensate for the loss of Vcx1-mediated Ca^{2+} sequestration in the *vcx1Δ* strain.

Consequently, we analysed glucose-induced TECC responses and pH changes in *gdt1Δ* strains (Fig. 7). At $\text{pH}_{\text{out}} 7$, pH_{cyt} and pH_{vac} responses were not significantly affected in the *gdt1Δ* strain (Fig. 7, B and C), while at $\text{pH}_{\text{out}} 5$, the glucose-induced cytosolic alkalization was faster and more pronounced resulting in a larger vacuolar H^+ gradient (Fig. 7, E and F). At $\text{pH}_{\text{out}} 7$, the peak amplitude of the TECC response in *gdt1Δ* strains was clearly enhanced but in the subsequent phase it relaxed to the same $[\text{Ca}^{2+}]_{\text{cyt}}$ as in the control wild-type cells, while at $\text{pH}_{\text{out}} 5$ the

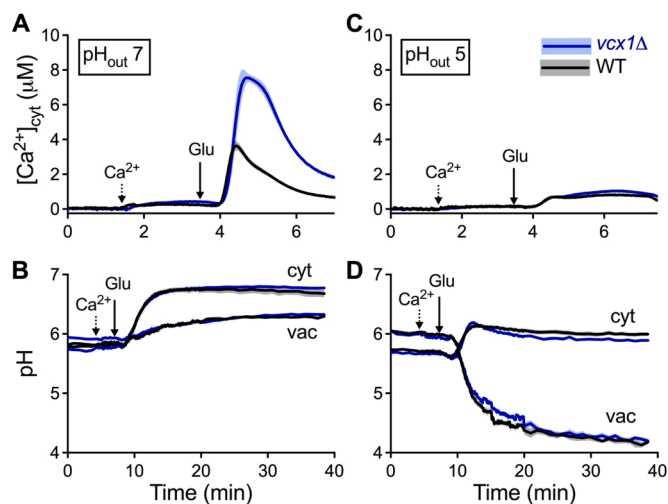


Fig. 6. Cytosolic $[Ca^{2+}]$ and pH changes in glucose-starved $vcx1\Delta$ yeast cells. (A and C) Averaged cytosolic Ca^{2+} transient (blue traces) in response to a 10 mM external $CaCl_2$ pulse (Ca^{2+} - first dotted arrow) followed by re-addition of glucose to a final concentration of 110 mM (Glu - second arrow) in $vcx1\Delta$ yeast cells kept at pH_{out} 7 (A) or 5 (C). For comparison, black traces show averaged cytosolic Ca^{2+} transient in control wild-type BY4741 cells (WT). Shaded areas either side of the Ca^{2+} transient trajectories reflect SEM. (B and D) Corresponding averaged cytosolic (blue traces labelled cyt) and vacuolar (blue traces labelled vac) pH in $vcx1\Delta$ yeast cells kept at pH_{out} 7 (B) or 5 (D). For comparison, overlaid black traces show averaged cytosolic and vacuolar pH changes in control wild-type BY4741 cells. Shaded areas either side of the pH data points reflect SEM.

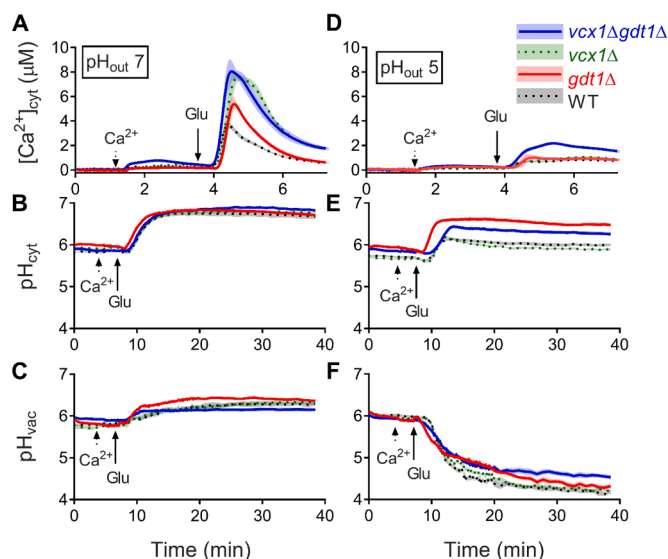


Fig. 7. Cytosolic $[Ca^{2+}]$ and pH changes in glucose-starved $gdt1\Delta$ and $vcx1\Delta gdt1\Delta$ yeast cells. (A and D) Averaged cytosolic Ca^{2+} transient in response to a 10 mM external $CaCl_2$ pulse (Ca^{2+} - first dotted arrow) followed by re-addition of glucose to a final concentration of 110 mM (Glu - second arrow) in $gdt1\Delta$ (red traces) and $vcx1\Delta gdt1\Delta$ (blue traces) yeast cells kept at pH_{out} 7 (A) or 5 (D). For comparison, black and green dotted traces show averaged cytosolic Ca^{2+} transient in control wild-type BY4741 (WT) and $vcx1\Delta$ cells, respectively. Shaded areas either side of the Ca^{2+} transient trajectories reflect SEM. Corresponding averaged cytosolic (B and E) and vacuolar (C and F) pH changes in $gdt1\Delta$ (red traces) and $vcx1\Delta gdt1\Delta$ (blue traces) yeast cells kept at pH_{out} 7 (B and C) or 5 (E and F). For comparison, overlaid black and green dotted traces show averaged cytosolic and vacuolar pH changes in control BY4741 and $vcx1\Delta$ cells, respectively. Shaded areas either side of the pH data points reflect SEM.

TECC response was not significantly affected (Fig. 7, A and D). When the $VCX1$ deletion was introduced in the $gdt1\Delta$ deletion strain ($vcx1\Delta gdt1\Delta$ - Fig. 7 A), the TECC response at pH_{out} 7 reached similar levels as those obtained in the single $vcx1\Delta$ mutant and pH changes were not affected. Compared to $gdt1\Delta$, $vcx1\Delta$ or wild-type cells, the TECC response at pH_{out} 5 in the $vcx1\Delta gdt1\Delta$ strain was clearly enhanced while the glucose-induced cytosolic alkalinization remained more pronounced (Fig. 7 D). These results therefore suggest that at pH_{out} 7, when cells are hyperpolarized and hence the glucose-induced cytosolic Ca^{2+} load is large, Ca^{2+} sequestration predominantly depends on $Vcx1$. However, at pH_{out} 5, when cells are depolarized and hence the glucose-induced cytosolic Ca^{2+} load is limited, both $Vcx1$ and $Gdt1$ equally contribute to Ca^{2+} sequestration. In this situation, loss of $Vcx1$ may be compensated by $Gdt1$, and vice versa. Finally, the effect of V-ATPase inhibition by CMA on the TECC response was tested in the $vcx1\Delta$, $gdt1\Delta$ and $vcx1\Delta gdt1\Delta$ strains (Fig. 8 - see also Fig. S6). First, at pH_{out} 7 (Fig. 8 upper panel), the peak TECC response was nearly doubled in vehicle-treated $vcx1\Delta$ and $vcx1\Delta gdt1\Delta$ cells in comparison to vehicle-treated wild-type cells while in vehicle-treated $gdt1\Delta$ cells the increase in peak TECC response was clearly less pronounced. In the presence of CMA, the peak TECC response significantly increased in wild-type and $gdt1\Delta$ cells but no further increase was observed for the $vcx1\Delta$ and $vcx1\Delta gdt1\Delta$ cells. Notably, in the presence of CMA the time course of recovery of the TECC response was significantly slowed in all strains. Together, these results support the idea that vacuolar Ca^{2+} reuptake through $Vcx1$ is the main Ca^{2+} sequestration mechanism in yeast cells

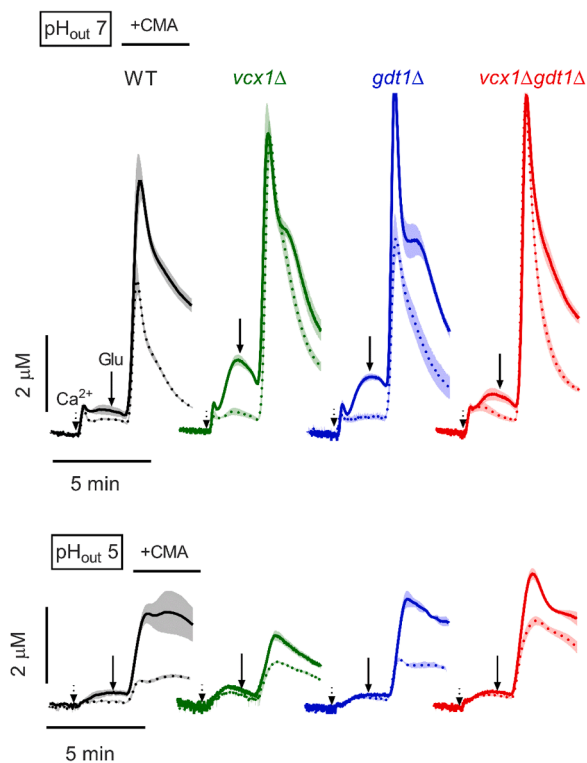


Fig. 8. Effect of the V-ATPase inhibitor Concanamycin A (CMA) on TECC responses. Effect of the inhibitor of vacuolar ATPase (V-ATPase) Concanamycin A (CMA) on cytosolic $[Ca^{2+}]$ changes during glucose re-addition to glucose-starved yeast cells kept at external pH 7 (upper panel) or 5 (lower panel). Averaged cytosolic Ca^{2+} transient in response to a 10 mM external $CaCl_2$ pulse (Ca^{2+} - first dotted arrow) followed by re-addition of glucose to a final concentration of 110 mM (Glu - second arrow) in wild-type (WT - black solid trace), $vcx1\Delta$ (green solid trace), $gdt1\Delta$ (blue solid trace) and $vcx1\Delta gdt1\Delta$ (red solid trace) yeast cells pretreated with 1 μ M CMA for 15 min. Overlaid dotted traces show averaged cytosolic Ca^{2+} transients in corresponding vehicle-treated control strains. Shaded areas either side of the Ca^{2+} transient trajectories reflect SEM.

and implicate the importance of V-ATPases in creating the pH gradient required for full Vcx1 (and Gdt1) activation [43, 65]. Additionally, at pH_{out} 7 the [Ca²⁺]_{cyt} increase associated with the addition of external Ca²⁺ was also clearly enhanced in the CMA-treated deletion strains. This finding indicates that this [Ca²⁺]_{cyt} increase is also largely controlled by the H⁺ gradient across the vacuolar and Golgi membrane and may thus reflect hampered organellar Ca²⁺ sequestration by Vcx1 and Gdt1 in CMA-treated cells. Second, at pH_{out} 5 (Fig. 8 lower panel), the appearance of small TECC responses was the result of membrane depolarization (Fig. 4) and hence limited glucose-induced Ca²⁺ influx. However, while at pH_{out} 7 the largest effects were observed in the deletion strains lacking Vcx1 (the *vcx1Δ* and *vcx1Δgdt1Δ* strains), at pH_{out} 5 the largest effects were associated with the deletion strains lacking Gdt1 (the *gdt1Δ* and *vcx1Δgdt1Δ* strains). This finding suggests that when the Ca²⁺ influx or cytosolic Ca²⁺ load is limited, Gdt1 plays a major role in Ca²⁺ sequestration. The finding that CMA further enhanced the peak TECC response in the *vcx1Δgdt1Δ* deletion strain at pH_{out} 5 suggests that imbalances caused by the combined deletion of *VCX1* and *GDT1* may be partly compensated by an increased or decreased expression or activity of other transports and regulatory proteins, but further experiments are required to test this possibility.

Finally, we also tested whether altered glucose uptake capacity in mutant strains would affect pH homeostasis. Based on the 2-NBDG fluorescence assay the uptake of glucose was estimated in the wild-type and mutant yeast strains at pH_{out} 5 and 7 (Fig. S 3). As compared with wild-type cells, we found no defects but rather an increase in glucose uptake in the mutant strains, which was especially pronounced in the *vcx1Δ* strain at pH_{out} 5. However, the finding that pH values recorded in *vcx1Δ* cells matched those obtained in wild-type cells (Fig. 6), strongly suggests that the observed increases in glucose uptake in the mutant strains do not directly govern pH homeostasis.

4. Discussion

Re-addition of glucose to glucose-starved yeast cells results in a variety of effects including a Transient Elevation of Cytosolic Ca²⁺ (TECC response) [12, 14, 15] and cytosolic/organelle pH change [34]. Although evidence exists for crosstalk between pH and Ca²⁺ homeostasis in eukaryotic cells including yeast [14, 39, 43, 45, 61, 66, 67], most studies have focused either on cytosolic Ca²⁺ alone or on cytosolic pH and our understanding of how these two are integrated is rather fragmented or based on circumstantial evidence. In this study, we optimized the aequorin-based bioluminescent assay for monitoring cytosolic Ca²⁺ changes in parallel with fluorescence reporter-based assays to monitor intracellular pH (cytosol and vacuole) and relative membrane potential changes to gain a better understanding of the links between pH, Ca²⁺ and membrane potential in *S. cerevisiae*.

The overall results show that glucose re-addition to glucose-starved yeast cells causes an increase in cytosolic Ca²⁺ ([Ca²⁺]_{cyt}; TECC response), clear changes in cytosolic (pH_{cyt}) and vacuolar (pH_{vac}) pH, and membrane hyperpolarization. At pH_{out} 7, large TECC responses (peak [Ca²⁺] of about 6 μM) were associated with alkalization of about 1.5 and 0.5 pH units for cytosol and vacuole, respectively. At pH_{out} 5, yeast cells were more depolarized and glucose re-addition induced small TECC responses (peak [Ca²⁺] of about 0.5 μM) associated with a cytosolic alkalization of about 0.5 pH units and a strong vacuolar acidification of about 2 pH units. Both at pH_{out} 7 and 5, the glucose-induced cytosolic alkalization was preceded with a small dip in pH of about 0.05 pH units. This initial cytosolic acidification has been attributed to the release of H⁺ during subsequent glucose phosphorylation steps [34], while the subsequent cytosolic alkalizing phase is thought to be mainly caused by a glucose-induced activation of the plasma membrane H⁺-ATPase (Pma1) [35].

Pma1 is considered to be the master determinant of cytosolic pH and plasma membrane potential [36], as a result of its electrogenic transport of H⁺. It was previously shown that in glucose-starved yeast cells Pma1

forms an inactive complex with acetylated tubulin [68, 69]. Ca²⁺ influx associated with glucose re-addition promotes activation of the Ca²⁺-dependent protease Lpx1, which then degrades the tubulin complex, making the pump accessible for phosphorylation and full activation [14, 66, 67]. However, in a first series of experiments we found that chelating extracellular Ca²⁺ greatly suppressed TECC responses at external pH 7 and 5 but not the accompanying pH changes. Additionally, when intracellular Ca²⁺ was chelated the TECC responses, but not the accompanying pH changes, were completely abolished. These findings indicate that in agreement with previous reports the TECC responses mainly rely on Ca²⁺ influx. However, the results also indicate that glucose-induced pH changes and hence glucose-induced Pma1 activation are not strictly Ca²⁺-dependent mechanisms. It should be noted that in the present work yeast cells were not pre-incubated with Ca²⁺ chelating solutions. Therefore, it is plausible that in the present experimental conditions the background activity of Lpx1 during starvation causes hydrolysis and dissociation of acetylated tubulin from Pma1, thereby rendering the pump immediately accessible for phosphorylation and full activation upon glucose re-addition.

To further investigate the contribution of Pma1, complementary experiments were performed in *pma1-007* mutant strain. The *pma1-007* mutant has a mutant promoter region that reduces its plasma membrane expression by about 50% and consequently this mutant displays an impaired capacity to pump H⁺ out of the cell [62]. Accordingly, glucose re-addition induced a slower and less pronounced cytosolic alkalization in the *pma1-007* mutant at pH_{out} 7. At pH_{out} 5, the cytosolic alkalization displayed a slower onset but the steady-state pH level was similar to control cells. These cytosolic pH changes were accompanied by a further alkalization shift in pH_{vac} at pH_{out} 7 and a marked basal and glucose-induced acidification at pH_{out} 5. The vacuolar acidification defect observed in both wild-type and *pma1-007* cells at pH_{out} 7 suggests a marked deficiency in vacuolar V-ATPase activity. Vacuolar acidification defects at elevated pH_{out} have been previously reported and the possibility of V-ATPase disassembly defects at alkaline extracellular pH was proposed [47]. However, co-localization analysis of Vma2-GFP, representing a peripheral subunit of the V-ATPase [70], and the vacuolar membrane dye FM4-64 revealed similar Pearson's colocalization coefficient values at pH_{out} 5 and 7. Moreover, the increase in colocalization coefficient value following glucose re-addition was in the same order of magnitude at pH_{out} 5 and 7. These findings therefore indicate that V-ATPase (re-)assembly was not impaired at pH_{out} 7. Since the glucose-induced vacuolar alkalization at pH_{out} 7 was similar in different proton-coupled transporter deletion strains, which besides *vcx1Δ* included strains lacking the Na⁺/H⁺ and K⁺/H⁺ exchanger Nhx1, the endoplasmic Ca²⁺/H⁺ antiporter Vnx1 or the vacuolar amino acid exchangers Avt3 and Avt4, we can also rule out the possibility that the vacuolar acidification defect at pH_{out} 7 is related to altered H⁺ exchange activity. Since ergosterol has been found to be critical for the V-ATPase function [71] and the expression of several genes involved in ergosterol biosynthesis is suppressed at more alkaline pH_{out} [72], the glucose-induced alkalized pH_{vac} at pH_{out} 7 may be related to reduced ergosterol biosynthesis. However, whether ergosterol levels were significantly reduced at pH_{out} 7 was not assessed in the present study and remains therefore to be investigated.

In contrast to the data obtained at pH_{out} 7, the *pma1-007* mutant displayed a prominent basal and glucose-induced hyperacidification at pH_{out} 5. The glucose-induced vacuolar hyperacidification likely reflects increased V-ATPase activity in the *pma1-007* mutant to limit the cytosolic acidification arising from loss of Pma1 activity. Consistent with these findings, vacuolar acidification was fully restored in aging mother yeast cells expressing the mutant *pma1-105* allele [73], suggesting that lower Pma1 activity leads to more cytosolic protons and higher V-ATPase activity. However, since vacuolar V-ATPases efficiently disassemble in response to glucose deprivation [42], the basal hyperacidification is difficult to reconcile with enhanced V-ATPase activity. In addition, CMA-treated *pma1-007* cells showed a similar basal

hyperacidification (data not shown). This suggests that apart from the V-ATPase other direct H^+ transport mechanisms may operate at low extracellular pH [74]. The larger $[Ca^{2+}]_{cyt}$ increase upon addition of external Ca^{2+} pulse at pH_{out} 5 in the *pma1-007* mutant was also particularly remarkable. The underlying mechanism is not clear, but one possibility to consider is that the basal vacuolar hyperacidification may impact on vacuolar Ca^{2+} homeostasis by stimulating Yvc1-mediated vacuolar Ca^{2+} release.

Another intriguing observation of the present study is that TECC responses were greatly suppressed at external pH 5. As TECC responses reflect the delicate balances between Ca^{2+} fluxes, this effect could be attributed to reduced Ca^{2+} influx or release, or enhanced Ca^{2+} uptake. The findings that glucose re-addition generated a H^+ gradient across the vacuolar membrane, which is about 2-3 fold larger at pH_{out} 5 (H^+ gradient of 1.74 and 0.75 pH units at pH_{out} 7 and 5, respectively), raises the possibility that vacuolar Ca^{2+} reuptake via Vcx1 is systematically enhanced at pH_{out} 5, thereby causing reduced TECC responses. In Vcx1 deletion strains, vacuolar H^+ gradients were preserved both at pH_{out} 7 and 5, indicating that Vcx1 activity contributes little to pH homeostasis. The finding that in *vcx1Δ* cells the TECC response displayed a higher peak and a subsequent elevated plateau at pH_{out} 7, is compatible with the idea that Vcx1 plays indeed a crucial role in Ca^{2+} dissipation [22]. At pH_{out} 5, TECC responses in the *vcx1Δ* deletion strain, however, remained small. This is not the result that would be expected if intracellular Ca^{2+} levels are tightly controlled by Vcx1. The magnitude of the TECC response depends not only on Ca^{2+} reuptake but also on the size of the Ca^{2+} influx. Since Pma1 generates hyperpolarizing current when activated, the pump activity may promote Ca^{2+} entry by increasing the electrochemical driving force for Ca^{2+} ions. The finding that TECC responses at external pH 7 were also strongly reduced in *pma1-007* mutants suggests that membrane potential may indeed determine Ca^{2+} influx and hence the amplitude of the TECC response. This was consecutively confirmed by a lower I580/I560 fluorescence ratio in *pma1-007* cells corresponding to partial depolarization of *pma1-007* cells. Further, we found that cells displayed significant higher I580/I560 ratios of DiS-C3 at more alkaline external pH and glucose re-addition consistently induced a I580/I560 ratio increase. Therefore, we propose that TECC responses mainly rely on Ca^{2+} influx from the external medium through an as-yet unidentified transport system, which was previously referred to as 'GIC' (Glucose Induced Calcium) [21] and is under direct control of the plasma membrane potential, which is primarily set by the Pma1 activity. Since glucose-induced activation of Pma1 also results in cytoplasmic alkalization and since pH interferes with protein function, we cannot exclude the possibility that cytosolic pH also influences GIC-related Ca^{2+} entry (with lower cytosolic pH associated with decreased Ca^{2+} influx).

In yeast the plasma membrane potential is mainly controlled by fluxes of H^+ and K^+ [75–77]. An increased cation influx, a decreased cation efflux or decreased Pma1 pump activity could explain why yeast cells at pH_{out} 5 are more depolarized than at pH_{out} 7. It has previously been shown that Pma1 stability sharply decreases at pH_{out} below 5.5 [78]. In addition, in our studies the membrane potentials were measured in yeast cells kept in a cation-free MES buffer solution, making it highly unlikely that increased cation influx governs membrane depolarization. This suggests that decreased Pma1 pump activity may underlie membrane depolarization at pH_{out} 5, similar to the depolarizing shift observed in *pma1-007* mutant cells. The observation that glucose re-addition induced a slower and smaller cytosolic alkalization at pH_{out} 5 as compared to pH_{out} 7 supports this hypothesis. Alternatively, differential expression or activity of K^+ leaks may be responsible. In yeast, several transporters have been identified that may contribute to K^+ efflux under K^+ -limiting conditions, including Na^+/K^+ ATPase Ena1 [79, 80], Na^+/H^+ or K^+/H^+ antiporter Nha1 [81], and K^+ channel Tok1 [82]. Ena1 has been found to be strongly activated under alkaline external pH [72]. Therefore, at more acidic pH_{out} decreased K^+ efflux via Ena1 during glucose starvation may result in substantial plasma

membrane depolarization.

The observations that despite the more favourable vacuolar H^+ gradient Vcx1 gene deletion had no impact on the small TECC responses at pH_{out} 5, while enhancing the large TECC responses at pH_{out} 7, further indicate that Vcx1 is very efficient to cope with large cytosolic Ca^{2+} transients (at pH_{out} 7). However, at lower cytosolic $[Ca^{2+}]$ other Ca^{2+} transporters, including the vacuolar Ca^{2+} -ATPase Pmc1, may dominate [43]. Furthermore, it has been shown that loss of Vcx1 function may partly be compensated by overexpression of Pmc1 [44]. In comparison, inhibiting V-ATPases with CMA dissipated the vacuolar H^+ gradient by 0.5 and 1.5 pH units at pH_{out} 7 and 5, respectively, thereby altering overall H^+/Ca^{2+} exchange-mediated Ca^{2+} sequestration. In support of the crucial role of Vcx1, TECC responses at pH_{out} 7 in CMA treated cells were enhanced. Surprisingly, CMA also clearly enhanced TECC responses at pH_{out} 5. Further analysis of CMA effects in *vcx1Δ*, *gdt1Δ* and *vcx1Δgdt1Δ* strains at pH_{out} 5 enabled us to identify the mechanisms of Ca^{2+} sequestration. The findings that TECC responses were slightly enhanced in both CMA-treated *vcx1Δ* and *gdt1Δ* strains and the observed additive effect in the CMA-treated *vcx1Δgdt1Δ* strain are consistent with perturbation of H^+/Ca^{2+} exchange as a consequence of H^+ gradient dissipation, and indicate that particularly at pH_{out} 5, the Golgi-localized H^+/Ca^{2+} transporter Gdt1 promotes Ca^{2+} dissipation following glucose re-addition. Notably, the CMA effect was more pronounced in *gdt1Δ* as compared to *vcx1Δ*. This difference may be attributed to overexpression of Pmc1 as a unique compensatory mechanism in *vcx1Δ* strains [43]. Furthermore, the TECC responses at pH_{out} 5 in CMA-treated *vcx1Δgdt1Δ* strain displayed increased $[Ca^{2+}]_{cyt}$ compared to CMA-treated wild-type cells. However, it is obvious that in contrast to CMA-treated *vcx1Δgdt1Δ* cells, some Vcx1 and Gdt1 activity may remain in CMA-treated wild-type cells, thereby lowering cytosolic $[Ca^{2+}]$. Finally, the glucose-induced cytosolic alkalization at both pH_{out} 5 and 7 in CMA-treated wild-type cells displayed slightly slower kinetics, suggesting that loss of V-ATPase activity also limits Pma1 activity. These results therefore support previous studies proposing that genetic or pharmacological inhibition of the V-ATPase is partly compensated by Pma1 downregulation [83, 84], reflecting Pma1 internalization through ubiquitin-mediated endocytosis [45, 85].

To summarize, cytosolic Ca^{2+} recordings in parallel with cytosolic and vacuolar pH measurements and estimates of membrane potential enabled us to better understand the interrelationship between pH and Ca^{2+} in yeast cells. Re-addition of glucose to glucose-starved yeast cells resulted in a Transient Elevation of Cytosolic Ca^{2+} (TECC response) associated with cytosolic/vacuolar pH and membrane potential changes. Our results support the idea that Pma1 plays a critical role in cytosolic pH homeostasis and its activity directly modulates membrane potential, while organelle acidification can be attributed to V-ATPase activity. The results provide evidence that Ca^{2+} influx is not a prerequisite for Pma1 pump activation but uncover that membrane hyperpolarization generated by Pma1 activation governs the Ca^{2+} influx. Additionally, a systematic analysis of yeast deletion strains allowed us to reveal an essential role for both Vcx1 and Gdt1 in the dissipation of intracellular Ca^{2+} .

Funding

This work was supported by a research grant of KU Leuven (C14-17-063) to J.W. and G.C. and of FWO-Vlaanderen (SBO grant S006617N) to J.W. T.-Y.M. was supported by a fellowship of the Taiwanese Government.

Appendix A. Supplementary data

See additional files ('CECA-D-21-00085 Revised supplementary figures' and 'CECA-D-21-00085 Revised supplementary tables')

CRedit authorship contribution statement

Tien-Yang Ma: Conceptualization, Methodology, Investigation, Formal analysis, Data curation, Visualization, Writing – original draft, Writing – review & editing. **Marie-Anne Deprez:** Methodology, Writing – review & editing. **Geert Callewaert:** Supervision, Conceptualization, Writing – original draft, Writing – review & editing, Data curation, Visualization. **Joris Winderickx:** Supervision, Conceptualization, Writing – original draft, Writing – review & editing, Project administration.

Declaration of Competing Interest

The authors declare that they have no known competing financial interests or personal relationships that could have appeared to influence the work reported in this paper.

Supplementary materials

Supplementary material associated with this article can be found, in the online version, at doi:10.1016/j.ceca.2021.102479.

References

- J. Humeau, J.M. Bravo-San Pedro, I. Vitale, et al., Calcium signaling and cell cycle: Progression or death, *Cell Calcium* 70 (2018) 3–15.
- M.J. Berridge, M.D. Bootman, P. Lipp, Calcium - a life and death signal, *Nature* 395 (1998) 645–648.
- M.J. Berridge, M.D. Bootman, H.L. Roderick, Calcium signalling: dynamics, homeostasis and remodelling, *Nat. Rev. Mol. Cell Biol.* 4 (2003) 517–529.
- C.R. Kahl, A.R. Means, Calcineurin Regulates Cyclin D1 Accumulation in Growth-stimulated Fibroblasts, *Mol. Biol. Cell* 15 (2004) 1833–1842.
- M.S. Cyert, J. Thorne, Regulatory subunit (CNB1 gene product) of yeast Ca²⁺/calmodulin-dependent phosphoprotein phosphatases is required for adaptation to pheromone, *Mol. Cell Biol.* 12 (1992) 3460–3469.
- E.M. Muller, E.G. Locke, K.W. Cunningham, Differential regulation of two Ca²⁺ influx systems by pheromone signaling in *Saccharomyces cerevisiae*, *Genetics* 159 (2001) 1527–1538.
- E.A. Espejo, The CRAZy Calcium Cycle, *Adv. Exp. Med. Biol.* 892 (2016) 169–186.
- T.K. Matsumoto, A.J. Ellmore, S.G. Cessna, et al., An osmotically induced cytosolic Ca²⁺ transient activates calcineurin signaling to mediate ion homeostasis and salt tolerance of *Saccharomyces cerevisiae*, *J. Biol. Chem.* 277 (2002) 33075–33080.
- A.F. Batiza, T. Schulz, P.H. Masson, Yeast respond to hypotonic shock with a calcium pulse, *J. Biol. Chem.* 271 (1996) 23357–23362.
- L. Viladevall, R. Serrano, A. Ruiz, et al., Characterization of the Calcium-mediated Response to Alkaline Stress in *Saccharomyces cerevisiae*, *J. Biol. Chem.* 279 (2004) 43614–43624.
- E. Peiter, M. Fischer, K. Sidaway, S.K. Roberts, D. Sanders, The *Saccharomyces cerevisiae* Ca²⁺ channel Gch1pMid1p is essential for tolerance to cold stress and iron toxicity, *FEBS Lett.* 579 (2005) 5697–5703.
- X. Li, J. Qian, C. Wang, et al., Regulating Cytoplasmic Calcium Homeostasis Can Reduce Aluminum Toxicity in Yeast, *PLoS One* 6 (2011) e21148.
- L.L. Ruta, V.C. Popa, I. Nicolau, et al., Calcium signaling mediates the response to cadmium toxicity in *Saccharomyces cerevisiae* cells, *FEBS Lett.* 588 (2014) 3202–3212.
- Y. Eilam, M. Othman, D. Halachmi, Transient increase in Ca²⁺ influx in *Saccharomyces cerevisiae* in response to glucose: effects of intracellular acidification and cAMP levels, *J. Gen. Microbiol.* 136 (1990) 2537–2543.
- Y. Eilam, M. Othman, Activation of Ca²⁺ influx by metabolic substrates in *Saccharomyces cerevisiae*: role of membrane potential and cellular ATP levels, *J. Gen. Microbiol.* 136 (1990) 861–866.
- R. Bagur, G. Hajnóczky, Intracellular Ca²⁺ Sensing: Its Role in Calcium Homeostasis and Signaling, *Mol. Cell* 66 (2017) 780–788.
- P. Pinton, T. Pozzan, R. Rizzuto, The Golgi apparatus is an inositol 1,4,5-tri-phosphate-sensitive Ca²⁺ store, with functional properties distinct from those of the endoplasmic reticulum, *EMBO J.* 17 (1998) 5298–5308.
- J. Strayle, T. Pozzan, H.K. Rudolph, Steady-state free Ca²⁺ in the yeast endoplasmic reticulum reaches only 10 microM and is mainly controlled by the secretory pathway pump pmr1, *EMBO J.* 18 (1999) 4733–4743.
- T. Dunn, K. Gable, T. Beeler, Regulation of cellular Ca²⁺ by yeast vacuoles, *J. Biol. Chem.* 269 (1994) 7273–7278.
- J. Nakajima-Shimada, H. Iida, F.I. Tsuji, Y. Anraku, Monitoring of intracellular calcium in *Saccharomyces cerevisiae* with an apoaequorin cDNA expression system, *Proc. Natl. Acad. Sci. U. S. A.* 88 (1991) 6878–6882.
- S. Groppi, F. Belotti, R.L. Brandão, E. Martegani, R. Tisi, Glucose-induced calcium influx in budding yeast involves a novel calcium transport system and can activate calcineurin, *Cell Calcium* 49 (2011) 376–386.
- A. Miseta, R. Kellermayer, D.P. Aiello, L. Fu, D.M. Bedwell, The vacuolar Ca²⁺/H⁺ exchanger Vcx1p/Hum1p tightly controls cytosolic Ca²⁺ levels in *S. cerevisiae*, *FEBS Lett.* 451 (1999) 132–136.
- J. Cui, J.A. Kaandorp, O.O. Ositelu, et al., Simulating calcium influx and free calcium concentrations in yeast, *Cell Calcium* 45 (2009) 123–132.
- P. D'Hooge, C. Coun, V. Van Eyck, et al., Ca²⁺ homeostasis in the budding yeast *Saccharomyces cerevisiae*: Impact of ER/Golgi Ca²⁺ storage, *Cell Calcium* 58 (2015) 226–235.
- D.P. Matheos, T.J. Kingsbury, U.S. Ahsan, K.W. Cunningham, Tcn1p/Crz1p, a calcineurin-dependent transcription factor that differentially regulates gene expression in *Saccharomyces cerevisiae*, *Genes Dev.* 11 (1997) 3445–3458.
- A.M. Stathopoulos, M.S. Cyert, Calcineurin acts through the CRZ1/TCN1-encoded transcription factor to regulate gene expression in yeast, *Genes Dev.* 11 (1997) 3432–3444.
- K.W. Cunningham, Acidic calcium stores of *Saccharomyces cerevisiae*, *Cell Calcium* 50 (2011) 129–138.
- K.W. Cunningham, G.R. Fink, Calcineurin-dependent growth control in *Saccharomyces cerevisiae* mutants lacking PMC1, a homolog of plasma membrane Ca²⁺ ATPases, *J. Cell Biol.* 124 (1994) 351–363.
- H.K. Rudolph, A. Antebi, G.R. Fink, et al., The yeast secretory pathway is perturbed by mutations in PMR1, a member of a Ca²⁺ ATPase family, *Cell* 58 (1989) 133–145.
- G. Dürr, J. Strayle, R. Plempner, et al., The medial-Golgi Ion Pump Pmr1 Supplies the Yeast Secretory Pathway with Ca²⁺ and Mn²⁺ Required for Glycosylation, Sorting, and Endoplasmic Reticulum-Associated Protein Degradation, *Mol. Biol. Cell* 9 (1998) 1149–1162.
- K.E. Barbara, T.M. Haley, K.A. Willis, G.M. Santangelo, The transcription factor Gcr1 stimulates cell growth by participating in nutrient-responsive gene expression on a global level, *Mol. Genet. Genomics* 277 (2007) 171–188.
- D. Demaegd, F. Foulquier, A.S. Colinet, et al., Newly characterized Golgi-localized family of proteins is involved in calcium and pH homeostasis in yeast and human cells, *Proc. Natl. Acad. Sci. U. S. A.* 110 (2013) 6859–6864.
- K.W. Cunningham, G.R. Fink, Calcineurin inhibits VCX1-dependent H⁺/Ca²⁺ exchange and induces Ca²⁺ ATPases in *Saccharomyces cerevisiae*, *Mol. Cell Biol.* 16 (1996) 2226–2237.
- S. Ramos, M. Balbín, M. Raposo, E. Valle, L.A. Pardo, The mechanism of intracellular acidification induced by glucose in *Saccharomyces cerevisiae*, *J. Gen. Microbiol.* 135 (1989) 2413–2422.
- V. Carmelo, H. Santos, I. Sá-Correia, Effect of extracellular acidification on the activity of plasma membrane ATPase and on the cytosolic and vacuolar pH of *Saccharomyces cerevisiae*, *Biochim. Biophys. Acta* 1325 (1997) 63–70.
- R. Serrano, M.C. Kielland-Brandt, G.R. Fink, Yeast plasma membrane ATPase is essential for growth and has homology with (Na⁺+K⁺), K⁺-and Ca²⁺-ATPases, *Nature* 319 (1986) 689–693.
- P. Erasó, M.J. Mazón, F. Portillo, Yeast protein kinase Ptk2 localizes at the plasma membrane and phosphorylates in vitro the C-terminal peptide of the H⁺-ATPase, *Biochim. Biophys. Acta* 1758 (2006) 164–170.
- A. Goossens, N. de La Fuente, J. Forment, R. Serrano, F. Portillo, Regulation of yeast H⁺-ATPase by protein kinases belonging to a family dedicated to activation of plasma membrane transporters, *Mol. Cell Biol.* 20 (2000) 7654–7661.
- J.L. Withee, R. Sen, M.S. Cyert, Ion tolerance of *Saccharomyces cerevisiae* lacking the Ca²⁺/CaM-dependent phosphatase (calcineurin) is improved by mutations in URE2 or PMA1, *Genetics* 149 (1998) 865–878.
- N.d.I. Fuente, A.M. Maldonado, F. Portillo, Yeast gene YOR137c is involved in the activation of the yeast plasma membrane H⁺-ATPase by glucose, *FEBS Lett.* 420 (1997) 17–19.
- M.S. Cyert, Calcineurin signaling in *Saccharomyces cerevisiae*: how yeast go crazy in response to stress, *Biochem. Biophys. Res. Commun.* 311 (2003) 1143–1150.
- K.J. Parra, C.-Y. Chan, J. Chen, *Saccharomyces cerevisiae* Vacuolar H⁺-ATPase Regulation by Disassembly and Reassembly: One Structure and Multiple Signals, *Eukaryot Cell* 13 (2014) 706–714.
- C. Förster, P.M. Kane, Cytosolic Ca²⁺ Homeostasis Is a Constitutive Function of the V-ATPase in *Saccharomyces cerevisiae*, *J. Biol. Chem.* 275 (2000) 38245–38253.
- G. Callewaert, P. D'Hooge, T.Y. Ma, et al., Decreased Vacuolar Ca²⁺ Storage and Disrupted Vesicle Trafficking Underlie Alpha-Synuclein-Induced Ca²⁺ Dysregulation in *S. cerevisiae*, *Front. Genet.* 11 (2020) 266.
- S.D. Velivela, P.M. Kane, Compensatory Internalization of Pma1 in V-ATPase Mutants in *Saccharomyces cerevisiae* Requires Calcium- and Glucose-Sensitive Phosphatases, *Genetics* 208 (2018) 655–672.
- P. Garrett-Engle, B. Moilanen, M.S. Cyert, Calcineurin, the Ca²⁺/Calmodulin-Dependent Protein Phosphatase, Is Essential in Yeast Mutants with Cell Integrity Defects and in Mutants That Lack a Functional Vacuolar H⁺-ATPase, *Mol. Cell Biol.* 15 (1995) 12.
- T.T. Diakov, P.M. Kane, Regulation of Vacuolar Proton-translocating ATPase Activity and Assembly by Extracellular pH, *J. Biol. Chem.* 285 (2010) 23771–23778.
- R. Mans, H.M. van Rossum, M. Wijsman, et al., CRISPR/Cas9: a molecular Swiss army knife for simultaneous introduction of multiple genetic modifications in *Saccharomyces cerevisiae*, *FEMS Yeast Res.* 15 (2015).
- T. Wilms, E. Swinnen, E. Eskes, et al., The yeast protein kinase Sch9 adjusts V-ATPase assembly/disassembly to control pH homeostasis and longevity in response to glucose availability, *PLoS Genet.* 13 (2017), e1006835.
- S. Büttner, L. Faes, W.N. Reichelt, et al., The Ca²⁺/Mn²⁺ ion-pump PMR1 links elevation of cytosolic Ca²⁺ levels to α -synuclein toxicity in Parkinson's disease models, *Cell Death Differ.* 20 (2013) 465–477.

- [51] R.H. Schiestl, R.D. Gietz, High efficiency transformation of intact yeast cells using single stranded nucleic acids as a carrier, *Curr. Genet.* 16 (1989) 339–346.
- [52] R. Tisi, S. Baldassa, F. Belotti, E. Martegani, Phospholipase C is required for glucose-induced calcium influx in budding yeast, *FEBS Lett.* 520 (2002) 133–138.
- [53] M. Bonora, C. Giorgi, A. Bononi, et al., Subcellular calcium measurements in mammalian cells using jellyfish photoprotein aequorin-based probes, *Nat. Protoc.* 8 (2013) 2105–2118.
- [54] D.G. Allen, J.R. Blinks, Calcium transients in aequorin-injected frog cardiac muscle, *Nature* 273 (1978) 509–513.
- [55] R. Orij, J. Postmus, A. Ter Beek, S. Brul, G.J. Smits, In vivo measurement of cytosolic and mitochondrial pH using a pH-sensitive GFP derivative in *Saccharomyces cerevisiae* reveals a relation between intracellular pH and growth, *Microbiology (Reading)* 155 (2009) 268–278.
- [56] C. Navarrete, S. Petrezsélyová, L. Barreto, et al., Lack of main K⁺ uptake systems in *Saccharomyces cerevisiae* cells affects yeast performance in both potassium-sufficient and potassium-limiting conditions, *FEMS Yeast Res.* 10 (2010) 508–517.
- [57] A. Peña, N.S. Sánchez, M. Calahorra, Estimation of the electric plasma membrane potential difference in yeast with fluorescent dyes: comparative study of methods, *J. Bioenerg. Biomembr.* 42 (2010) 419–432.
- [58] J. Schindelin, I. Arganda-Carreras, E. Frise, et al., Fiji: an open-source platform for biological-image analysis, *Nat. Methods* 9 (2012) 676–682.
- [59] S. Bolte, F.P. Cordelières, A guided tour into subcellular colocalization analysis in light microscopy, *J. Microsc.* 224 (2006) 213–232.
- [60] A. Roy, A.D. Dement, K.H. Cho, J.H. Kim, Assessing glucose uptake through the yeast hexose transporter 1 (Hxt1), *PLoS One* 10 (2015), e0121985.
- [61] M.J.M. Trópia, A.S. Cardoso, R. Tisi, et al., Calcium signaling and sugar-induced activation of plasma membrane H⁺-ATPase in *Saccharomyces cerevisiae* cells, *Biochem. Biophys. Res. Commun.* 343 (2006) 1234–1243.
- [62] Z. Porat, N. Wender, O. Erez, C. Kahana, Mechanism of polyamine tolerance in yeast: novel regulators and insights, *Cell. Mol. Life Sci.* 62 (2005) 3106–3116.
- [63] J. Plášek, D. Gášková, Complementary Methods of Processing diS-C3(3) Fluorescence Spectra Used for Monitoring the Plasma Membrane Potential of Yeast: Their Pros and Cons, *J. Fluoresc.* 24 (2014) 541–547.
- [64] P.M. Kane, Regulation of V-ATPases by reversible disassembly, *FEBS Lett.* 469 (2000) 137–141.
- [65] N.A. Snyder, C.P. Stefan, C.T. Soroudi, A. Kim, C. Evangelista, K.W. Cunningham, H⁺ and Pi Byproducts of Glycosylation Affect Ca²⁺ Homeostasis and Are Retrieved from the Golgi Complex by Homologs of TMEM165 and XPR1, *G3 (Bethesda)* 7 (2017) 3913–3924.
- [66] M.B.P. Pereira, R. Tisi, L.G. Fietto, et al., Carbonyl cyanide m-chlorophenylhydrazone induced calcium signaling and activation of plasma membrane H⁺-ATPase in the yeast *Saccharomyces cerevisiae*: Carbonyl cyanide m-chlorophenylhydrazone, *FEMS Yeast Res.* 8 (2008) 622–630.
- [67] D.D. Castanheira, E.P. Santana, F. Godoy-Santos, R.H.S. Diniz, Lpx1p links glucose-induced calcium signaling and plasma membrane H⁺-ATPase activation in *Saccharomyces cerevisiae* cells, *FEMS Yeast Res.* 18 (2018).
- [68] A.N. Campetelli, G. Previtali, C.A. Arce, H.S. Barra, C.H. Casale, Activation of the plasma membrane H⁺-ATPase of *Saccharomyces cerevisiae* by glucose is mediated by dissociation of the H⁺-ATPase-acetylated tubulin complex, *FEBS J.* 272 (2005) 5742–5752.
- [69] A.N. Campetelli, N.E. Monesterolo, G. Previtali, et al., Activation of H⁺-ATPase by glucose in *Saccharomyces cerevisiae* involves a membrane serine protease, *Biochim. Biophys. Acta* 1830 (2013) 3593–3603.
- [70] T.H. Stevens, M. Forgac, Structure, function and regulation of the vacuolar H⁺-ATPase, *Annu. Rev. Cell Dev. Biol.* 13 (1997) 779–808.
- [71] Y.-Q. Zhang, S. Gamarra, G. Garcia-Effron, S. Park, D.S. Perlin, R. Rao, Requirement for Ergosterol in V-ATPase Function Underlies Antifungal Activity of Azole Drugs, *PLoS Pathog.* 6 (2010), e1000939.
- [72] C. Casado, A. González, M. Platara, A. Ruiz, J. Ariño, The role of the protein kinase A pathway in the response to alkaline pH stress in yeast, *Biochem. J.* 438 (2011) 523–533.
- [73] K.A. Henderson, A.L. Hughes, D.E. Gottschling, Mother-daughter asymmetry of pH underlies aging and rejuvenation in yeast, *Elife* 3 (2014) e03504.
- [74] P.J. Plant, M.F. Manolson, S. Grinstein, N. Demaurex, Alternative mechanisms of vacuolar acidification in H⁺-ATPase-deficient yeast, *J. Biol. Chem.* 274 (1999) 37270–37279.
- [75] D.S. Perlin, C.L. Brown, J.E. Haber, Membrane potential defect in hygromycin B-resistant pma1 mutants of *Saccharomyces cerevisiae*, *J. Biol. Chem.* 263 (1988) 18118–18122.
- [76] L. Maresova, E. Urbankova, D. Gaskova, H. Sychrova, Measurements of plasma membrane potential changes in *Saccharomyces cerevisiae* cells reveal the importance of the Tok1 channel in membrane potential maintenance, *FEMS Yeast Res.* 6 (2006) 1039–1046.
- [77] R. Madrid, M.J. Gómez, J. Ramos, A. Rodríguez-Navarro, Ectopic potassium uptake in trk1 trk2 mutants of *Saccharomyces cerevisiae* correlates with a highly hyperpolarized membrane potential, *J. Biol. Chem.* 273 (1998) 14838–14844.
- [78] V. Carmelo, P. Bogaerts, I. Sá-Correia, Activity of plasma membrane H⁺-ATPase and expression of PMA1 and PMA2 genes in *Saccharomyces cerevisiae* cells grown at optimal and low pH, *Archives of Microbiology* 166 (1996) 315–320.
- [79] J. Zahrádka, H. Sychrová, Plasma-membrane hyperpolarization diminishes the cation efflux via Nha1 antiporter and Ena ATPase under potassium-limiting conditions, *FEMS Yeast Res.* 12 (2012) 439–446.
- [80] R. Haro, B. Garcíadeblas, A. Rodríguez-Navarro, A novel P-type ATPase from yeast involved in sodium transport, *FEBS Lett.* 291 (1991) 189–191.
- [81] M.A. BaAuelos, H. Sychrová, C. Bleykasten-Grosshans, J.L. Souciet, S. Potier, The Nha1 antiporter of *Saccharomyces cerevisiae* mediates sodium and potassium efflux, *Microbiology (Reading)* 144 (Pt 10) (1998) 2749–2758.
- [82] C. Fairman, X.-L. Zhou, C. Kung, Potassium Uptake Through the TOK1 K⁺ Channel in the Budding Yeast, *J. Membr. Biol.* 168 (1999) 149–157.
- [83] G.A. Martínez-Muñoz, P. Kane, Vacuolar and plasma membrane proton pumps collaborate to achieve cytosolic pH homeostasis in yeast, *J. Biol. Chem.* 283 (2008) 20309–20319.
- [84] M. Tarsio, H. Zheng, A.M. Smardon, G.A. Martínez-Muñoz, P.M. Kane, Consequences of loss of Vph1 protein-containing vacuolar ATPases (V-ATPases) for overall cellular pH homeostasis, *J. Biol. Chem.* 286 (2011) 28089–28096.
- [85] A.M. Smardon, P.M. Kane, Loss of vacuolar H⁺-ATPase activity in organelles signals ubiquitination and endocytosis of the yeast plasma membrane proton pump Pma1p, *J. Biol. Chem.* 289 (2014) 32316–32326.